AD-A250 983

J PAGE

Form Approved
OMB No. 0704-0188

Public repor
gathering ar
collection of
Davis Highw

our per response, including the time for reviewing instructions, searching existing data sources,
tion of information. Send comments regarding this burden estimate or any other aspect of this
ton Headquarters Services, Directorate for information Operations and Reports, 1215 Jefferson
ent and Budget, Paperwork Reduction Project (0704-0188), Washington, DC 20503.

1. AGENCY USE ONLY (Leave blank)	2. REPORT DATE	3. REPORT TYPE AND DATES COVERED
	May 1992	Final Report 5/1/89 - 1/31/92

4. TITLE AND SUBTITLE

The Synthesis and Characterization of Tribophysical Layers on Diamond and Silicon Carbide Surfaces

5. FUNDING NUMBERS

61102F 2303/A2

6. AUTHOR(S)

John T. Yates, Jr.

7. PERFORMING ORGANIZATION NAME(S) AND ADDRESS(ES)

University of Pittsburgh
Department of Chemistry
Pittsburgh, PA 15260

8. PERFORMING ORGANIZATION REPORT NUMBER

AFOSR-TR- 92 0444

9. SPONSORING / MONITORING AGENCY NAME(S) AND ADDRESS(ES)

AFOSR/NC
Bolling AFB, DC 20332-6448

10. SPONSORING / MONITORING AGENCY REPORT NUMBER

AFOSR-89-0364

11. SUPPLEMENTARY NOTES

12a. DISTRIBUTION / AVAILABILITY STATEMENT

Approved for public release; distribution is unlimited

12b. DISTRIBUTION CODE

13. ABSTRACT *(Maximum 200 words)*

A new ultrahigh vacuum apparatus, dedicated to the study of the surface chemistry of diamond single crystals, has been completed and the first scientific experiments have been done. This apparatus incorporates XPS, LEED, ESDIAD, HREELS, and TPD facilities for the study of the fluorination and hydrogenation of diamond single crystals. The apparatus is being employed for studies of atomic hydrogen/deuterium adsorption on diamond(100) in initial experiments prior to the use of XeF_2 as a fluorinating agent. It is proposed to study the formation of CH_x and CF_x surface species, the thermal desorption products from these species, the resistance to oxidation by these species, and the functionalization of the diamond surface by fluorinated molecules such as C_2F_4, NF_3, and CF_3CF.

Collaborative AFM studies of diamond AFM tips sliding over our diamond(100) single crystal are underway, in work being done with Dr. Gary McClelland at IBM Almaden. Frictional studies completed on the non-modified surface will be compared to studies on fluorinated diamond(100).

14. SUBJECT TERMS

15. NUMBER OF PAGES 42

16. PRICE CODE

17. SECURITY CLASSIFICATION OF REPORT	18. SECURITY CLASSIFICATION OF THIS PAGE	19. SECURITY CLASSIFICATION OF ABSTRACT	20. LIMITATION OF ABSTRACT
UNCLASSIFIED	UNCLASSIFIED	UNCLASSIFIED	

UNIVERSITY OF PITTSBURGH

DEPARTMENT OF CHEMISTRY

submitted to:

Air Force Office of Scientific Research

FINAL REPORT

Entitled

THE SYNTHESIS AND CHARACTERIZATION OF TRIBOPHYSICAL LAYERS ON DIAMOND AND SILICON CARBIDE SURFACES

AFOSR-89-0364

(Time Period: 1988 to 1991)

PRINCIPAL INVESTIGATOR

John T. Yates, Jr.
R.K. Mellon Professor of Chemistry
Director, Pittsburgh Surface Science Center

John T. Yates, Jr.

Surface Science Center
Department of Chemistry
University of Pittsburgh
Pittsburgh, PA 15260
412-624-8320

Table of Contents

Page

Surface Chemistry of Diamond Single Crystals

John T. Yates, Jr.

Surface Science Center
Department of Chemistry
University of Pittsburgh
Pittsburgh, PA 15260
412-624-8320

Abstract

A new ultrahigh vacuum apparatus, dedicated to the study of the surface chemistry of diamond single crystals, has been completed and the first scientific experiments have been done. This apparatus incorporates XPS, LEED, ESDIAD, HREELS, and TPD facilities for the study of the fluorination and hydrogenation of diamond single crystals. The apparatus is being employed for studies of atomic hydrogen/deuterium adsorption on diamond(100) in initial experiments prior to the use of XeF_2 as a fluorinating agent. It is proposed to study the formation of CH_x and CF_x surface species, the thermal desorption products from these species, the resistance to oxidation by these species, and the functionalization of the diamond surface by fluorinated molecules such as C_2F_4, NF_3, and CF_3OF.

Collaborative AFM studies of diamond AFM tips sliding over our diamond(100) single crystal are underway, in work being done with Dr. Gary McClelland at IBM Almaden. Frictional studies completed on the non-modified surface will be compared to studies on fluorinated diamond(100).

I. Introduction

A. Study of Single Crystal Diamond Surface Chemistry

This project is focussed on understanding the surface chemistry of diamond single crystals, using modern methods of surface science to gain information at the atomic level.

The primary objective is to gain understanding about the fluorination of the diamond surface using various chemical routes to the production of fluorine-containing surface groups. In addition to the production and characterization of the fluorinated diamond surface, studies of its thermal and chemical stability are planned. This information is expected to be of importance in the lubrication of diamond surfaces for high technology applications. In addition, although not one of the primary goals, the information about the fluorine-induced surface chemistry of diamond may also relate to the chemistry involved in the growth of diamond films [1].

Auxiliary studies of the hydrogenation of diamond are also underway, as it will be instructive to compare the fluorinated and hydrogenated surfaces.

Two additional activities related to diamond surface chemistry have been carried out under AFOSR support during the first 25 months of the project. One involves exploratory AFM (atomic force microscopy) studies of the crystal topography and the frictional character of diamond sliding on diamond. This work was carried out collaboratively at the IBM Alamaden Laboratories, using a graduate student from Pittsburgh working with Dr. Gary McClelland. The second activity involves the publication of a data base of research papers and other published information entitled "Selected Biblography-Diamond Surface Chemistry", by V.S. Smentkowski and J.T. Yates, Jr. This has been disseminated as a Technical Report by AFOSR as Project No. 2303, Task A2.

The project has been funded since April 15, 1989. During this time, significant progress has been made, and a dedicated ultrahigh vacuum system has been constructed and tested at The University of Pittsburgh. The apparatus has met all design specifications, and the first scientific measurements have been made on diamond(100).

B. Completion of Studies of the Structure and Dynamics of Adsorbates on Metal Single Crystals

The work on diamond follows a successful project supported by AFOSR for about 9 years in which the digital ESDIAD method was developed and applied to a wide range of studies of the bonding and dynamics of chemisorbed species on single crystal metal surfaces. During the first 25 months' work on the diamond project, we have been completing our digital ESDIAD activities, and this proposal will also report on these last results. One of the most outstanding results from the project has been the production of a definitive review on the subject of electron stimulated desorption, entitled "Electron Stimulated Desorption: Principles and Applications", by R.D. Ramsier and J.T. Yates, Jr., Surface Science Reports, Vol. 12, Nos. 6-8 (1991), pp. 243-378. This review covers recent theory and experiment, and contains over 1000 references (from 1918-1990), organized by subject, by adsorbate and surface, and by leading author. It is anticipated that the review, which is the most complete of 66 reviews on electron stimulated desorption published to date, will be widely used throughout the field for many years.

II. Outline of Progress in Diamond Project

A. Ultrahigh Vacuum Apparatus

The ultrahigh vacuum apparatus shown in Figure 1a and 1b has been completed and is routinely operating at 7×10^{-11} torr. This apparatus was designed and constructed at the University of Pittsburgh from stainless steel tubing and commercially obtained spectrometers and mechanical components. It features a full range of facilities for the investigation of the chemical and physical properties of diamond surfaces, and is fully dedicated to research on diamond.

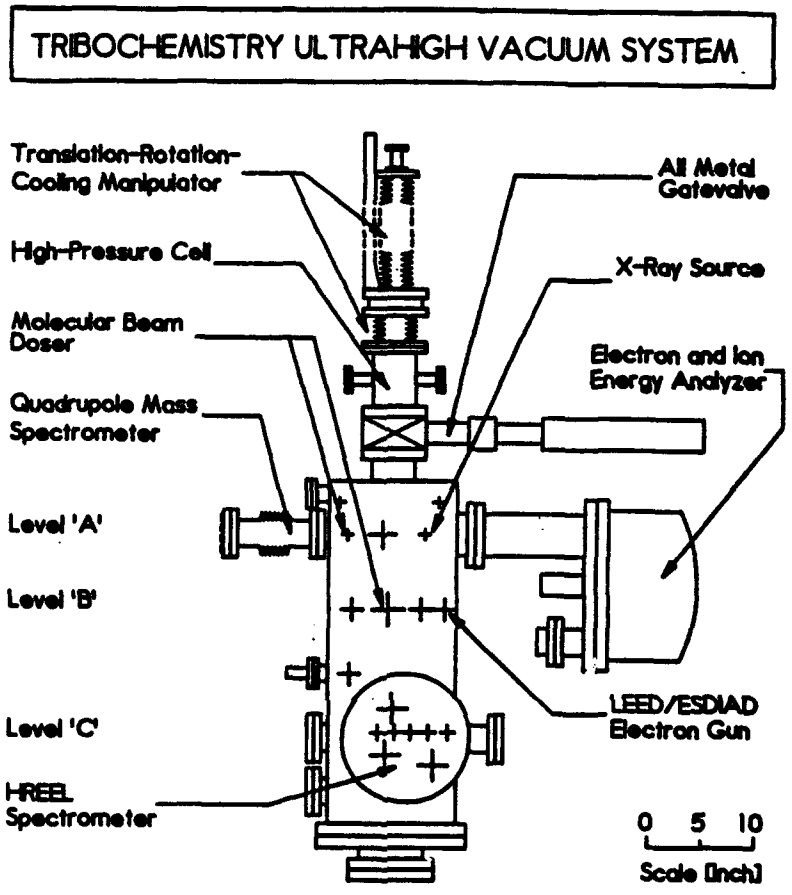

Figure 1a. Tribochemistry Ultrahigh Vacuum System.

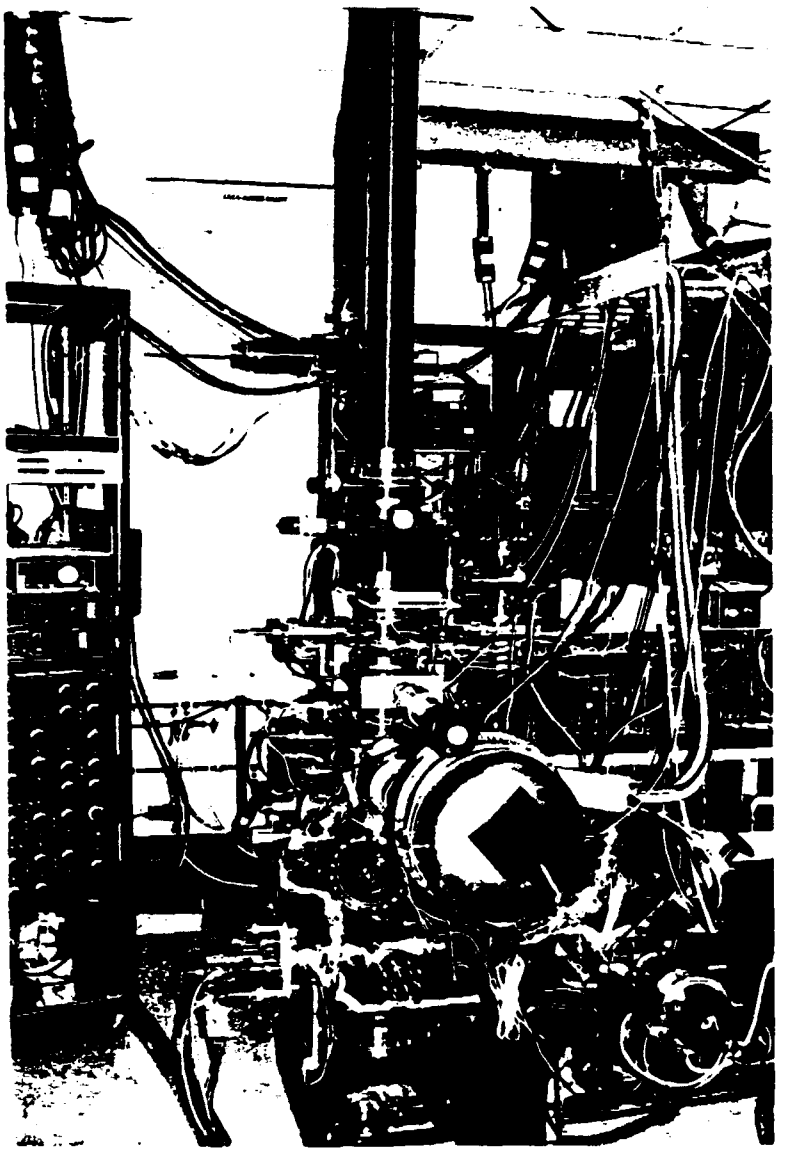

Figure 1b. Photograph of Ultrahigh Vacuum System for Studies of Diamond Surface Chemistry.

The basic features of the apparatus are described below:

- HREEL Spectrometer- operating in a magnetically shielded environment for the investigation of the vibrational characteristics of diamond surfaces containing adsorbed species. The instrument delivers an elastic beam count rate of 4×10^4/s at a resolution of 65 cm^{-1} in preliminary investigations of the diamond crystal surface.

- XPS Spectrometer- Operating with Al K_α and Mg K_α X-ray sources. Spectrometer energy scale can routinely be cross calibrated with atomically clean Au and Cu standards, present on a separate manipulator in the chamber.

- LEED/ESDIAD analyzer- Operating with a microchannel-plate detector amplifier to minimize possible electron beam damage to diamond surface or to adsorbed layers. Typically, 10 nA electron beam currents are employed.

- Quadrupole Mass Spectrometer- Apertured instrument which samples only the central region of the diamond crystal in thermal desorption measurements at a 1 mm spacing from the crystal. In addition, by opening a shield porthole, the mass spectrometer may be used to measure the composition and pressure of gases within the entire vacuum chamber. The aperture to the shielded mass spectrometer is electrically biased at negative potential to retard thermionically-produced electrons from the ionization source, preventing spurious electron beam damage to the diamond crystal surface or to adsorbates on the diamond surface.

- Molecular Beam Dosers- Two calibrated beam dosers supply a known flux of gases to the diamond crystal. In the case of the doser for XeF_2, the aperture of the doser exactly corresponds to the 6mm x 6mm cross section of the diamond crystal and the doser can be translated up to the front face of the crystal using a micrometer adjustment. These dosers minimize exposure of the vacuum system to deleterious gases, preserving vacuum and electron multiplier detectors.

- High Pressure Cell- An auxiliary chamber, separately pumped, for treatment of the diamond crystal under extreme conditions. The chamber contains a hot tungsten filament source for production of atomic hydrogen, and CaF_2 or sapphire ultrahigh vacuum windows for ultra-violet photolysis of adsorbates or gases in front of the diamond crystal. Wavelength selection, using filters and a high pressure focused Hg arc, is carried out with absolutely calibrated photon fluxes. Photolysis of adsorbates on the diamond surface is also possible at this level as well as at other levels in the system. The high pressure chamber is sealed with an all metal gate valve to avoid gas contamination from Viton O-rings upon squeezing for closure.

- Translation-Rotation-Cooling Manipulator- This is a unique device containing a vacuum-jacketed sample holder tube which can hold liquid nitrogen for long periods. The vacuum jacket, combined with a small bellows at the top, prevents vertical motion of the diamond crystal due to thermal expansion as the liquid nitrogen level changes in the support tube. Full rotation using differentially pumped seals plus 1 meter vertical translation and micrometer-driven horizontal translation are features of the manipulator.

- Ultrahigh Vacuum Pumping- The system contains three turbopumps, a 360 L/s ion pump, and a titanium sublimation pump. The main turbopump is backed by an oil diffusion pump for maximum pumping speed.

A photograph of our homebuilt microchannelplate LEED/ESDIAD analyzer is shown in Figure 2. This analyzer is translatable into the UHV chamber when the diamond crystal is in position, and may be withdrawn during movement of the diamond in the up-down direction.

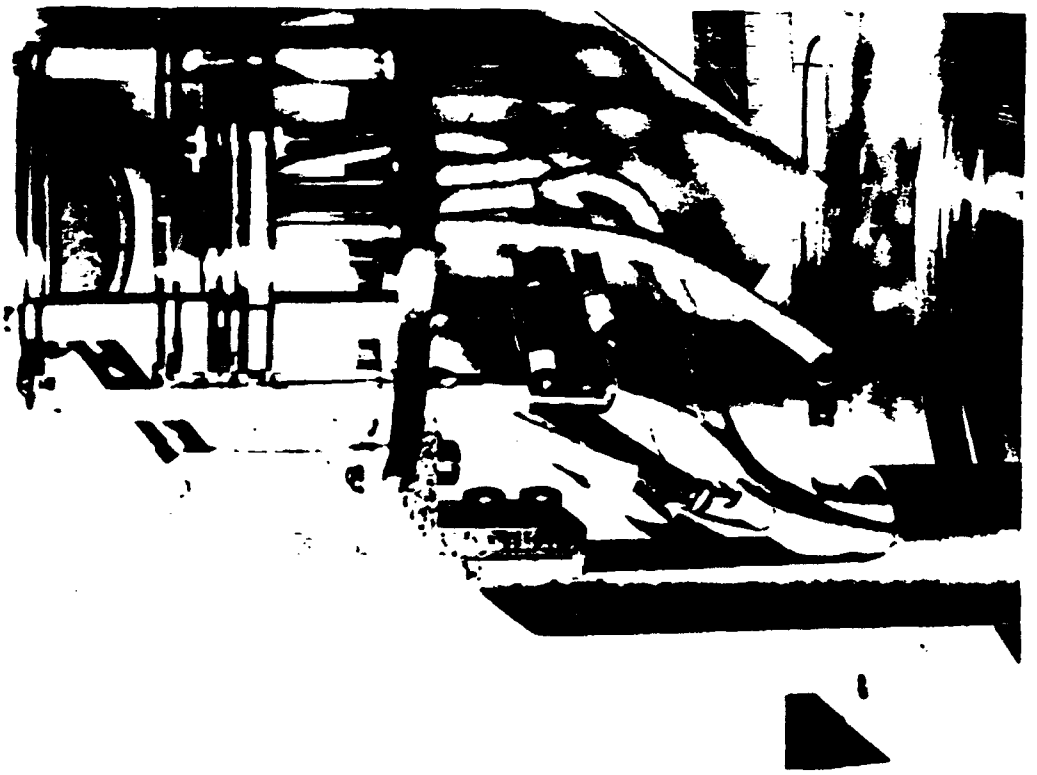

Figure 2. Homebuilt LEED/ESDIAD Analyzer Showing Hemispherical Grids, Microchannelplate Detector, and Electron Gun Drift Tube Penetrating the Grids.

B. Preparation of IIa Diamond Crystal.

The diamond(100) surface has been chosen for our first investigations. Figure 3 shows the configuration of the single crystal and the Laue X-ray pattern of the oriented diamond crystal. The diamond crystal has been specially prepared with mounting slots on two edges and with tiny thermocouple holes laser drilled from the edges into the center of the 0.5 mm thick crystal.

The Laue X-ray pattern indicates that the diamond is oriented to within about 1.0° of the (100) direction. As will be shown later, AFM measurements indicate that the diamond exposes large regions which are atomically flat.

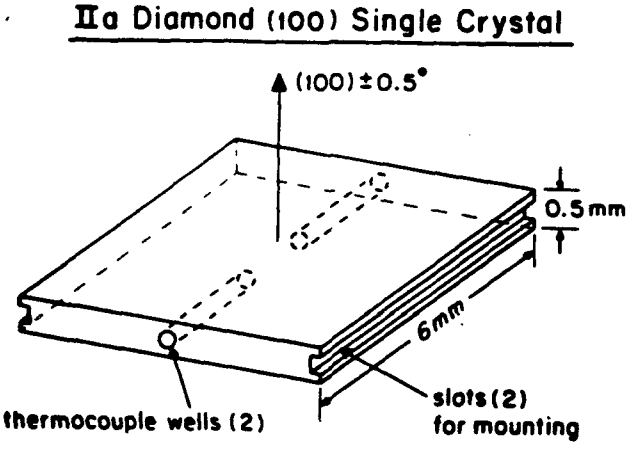

Figure 3. The Diamond(100) Single Crystal.

The use of two embedded thermocouples permits two experimental measurements of the diamond heating characteristics- (1) the temperature uniformity across a 2 mm wide region in the center of the diamond crystal; and (2) the temperature of the diamond itself rather than the temperature of a support surface in contact with the diamond. It will be shown below that this is a very important feature of our experimental procedure.

The IIa natural diamond is more common than the B-doped IIb diamond and hence less costly. It has a low doping level and a high electrical resistivity. Thus, arrangements for inducing diamond photoconductivity have been made at critical levels in the vacuum system by provision of ultraviolet transmitting windows.

C. Mounting and Heating of Diamond.

Figure 4 illustrates the method we are employing for

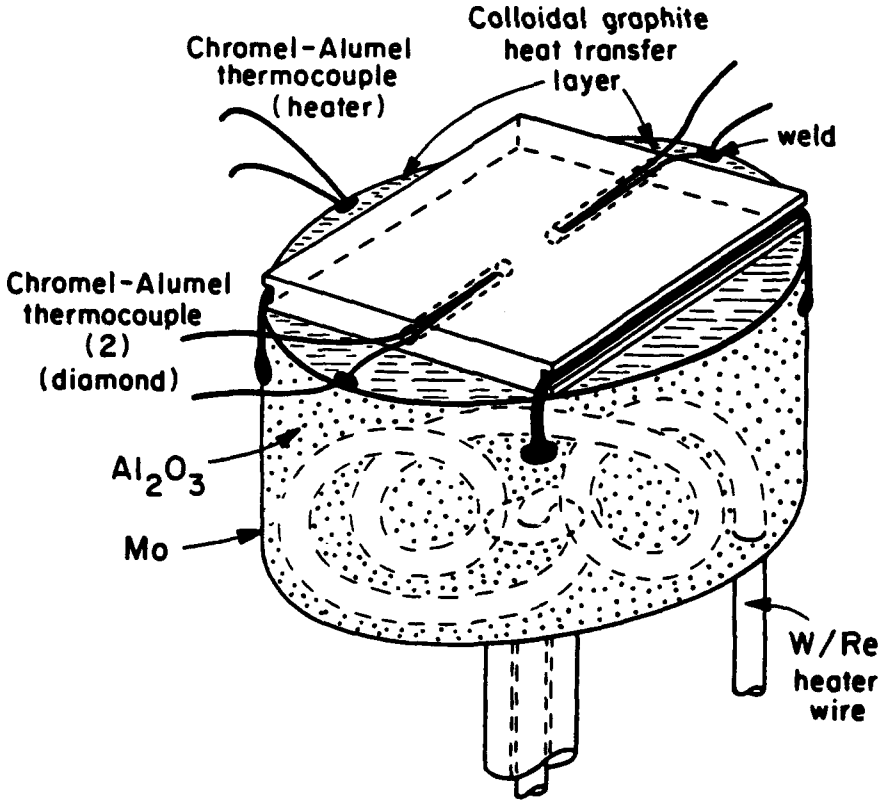

Figure 4. Mounting for Diamond Crystal

heating the diamond. The diamond is mounted on a button heater with a Mo casing. The top surface of the case has been polished with diamond paste. The diamond is coated on its back side with a burnished coat of colloidal graphite, and the two surfaces are contacted to make a good thermal junction.

The diamond is strapped with Ta mounting wires which fit through the slots on the two edges and which are welded to the outside of the button heater, under slight tension. The thermocouple wires enter the tiny holes and penetrate deep into the center of the crystal. One leg of each thermocouple wire is spot welded to the button heater for security and also for heat stationing of the thermocouple. A third thermocouple is welded to the outer surface of the button heater, and supplies information about the temperature differences which exist between the diamond itself and the surface of the button heater.

The temperature range which can be achieved is from 100 K to 1625 K.

It should be noted that the front surface of the diamond crystal is not exposed to hot metallic surfaces in the mounting arrangement shown in Figure 4. This prevents the transfer of evaporated metal or metal oxides to the diamond surface. This is a critical design feature, since cleaning these substances from the surface inside the vacuum system would not be easily carried out- for example, ion bombardment sputtering would convert the diamond surface to graphite.

A special electronic temperature programmer has been constructed to reproducibly program the diamond crystal at various desired rates of heating. The programmer will also maintain the diamond crystal at any desired temperature with a precision of about 1 K using its feedback circuitry [2].

Figure 5 illustrates the orientation of the diamond as it is mounted on the manipulator. The long axis of the diamond is mounted vertically in order to accommodate the 5mm high focused electron beam of the HREEL spectrometer. This permits a 2mm error in the vertical position of the crystal to be without consequence. In addition, as shown in Figure 5, the apertured mass spectrometer, placed about 1mm from the diamond surface, samples thermal desorption only from the central portion of the crystal.

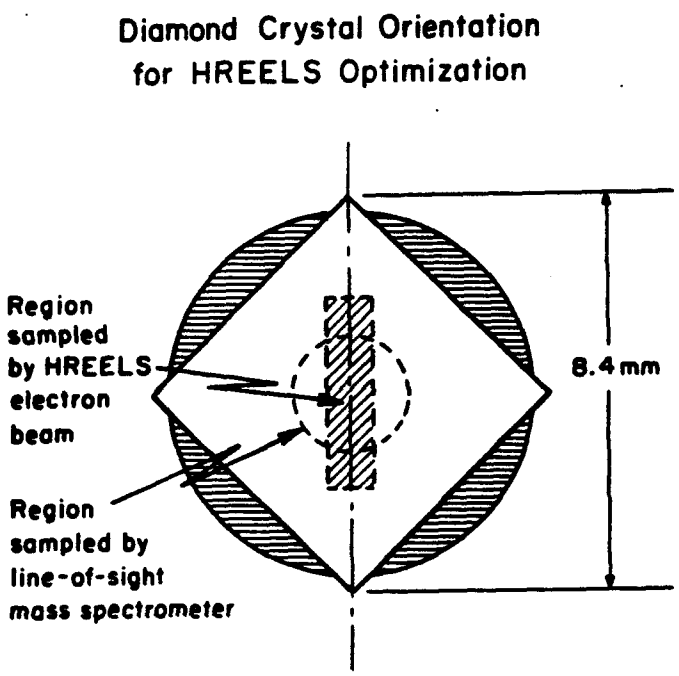

Figure 5. Azimuthal Orientation of Diamond Crystal in UHV Apparatus.

D. Thermal Behavior of Diamond

Figure 6 indicates the uniformity of heating which has been measured for the diamond crystal using a comparison between the two embedded thermocouples over a range of diamond temperatures. The temperature difference is minimal (<5 K) over this temperature range. This would be expected for a material possessing the high thermal conductivity of a diamond single crystal, and the temperature differences probably represent the error in making thermocouple temperature measurements.

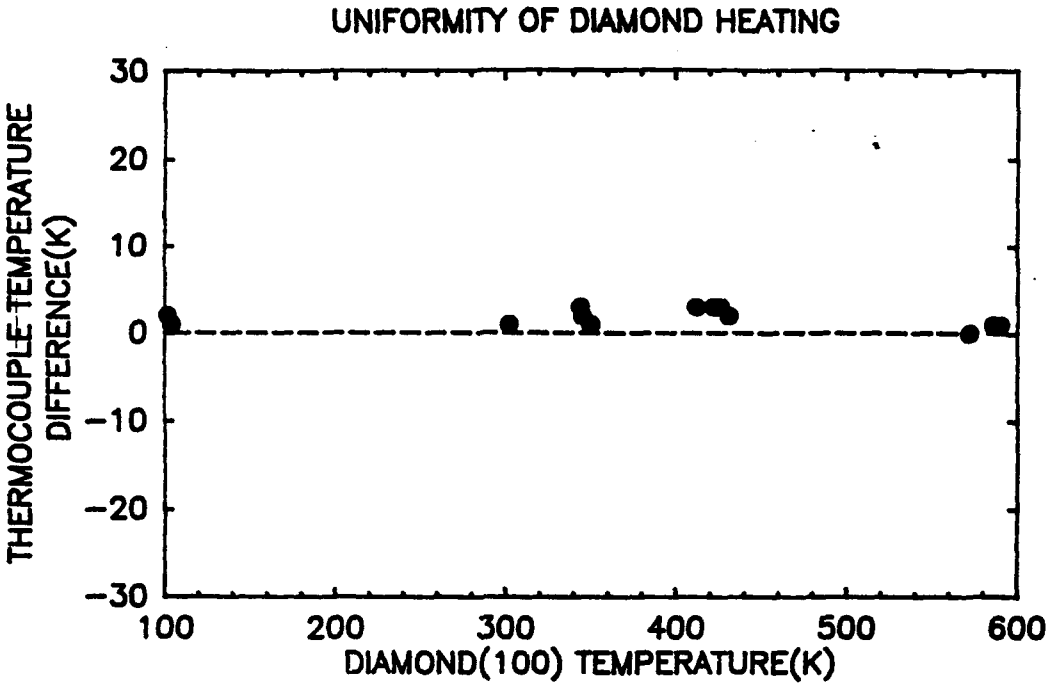

Figure 6. Comparison of Two Embedded Thermocouples

E. Programmed Heating of Diamond- Comparison of Diamond Temperature with Button Heater Temperature.

Figure 7 shows an experiment in which the temperature programmer was employed to heat the diamond crystal; both the temperature of the diamond and the temperature of the button heater surface were simultaneously monitored. For ideal conditions, where both temperatures are equal, a 45° line would be expected, as shown by the dashed line. It is observed on heating that the true diamond temperature always lags behind the temperature of the button heater surface. This difference approaches 100 K for higher temperatures. THIS TYPE OF ERROR IS SIGNIFICANT IN STUDIES OF THE THERMAL PROPERTIES OF DIAMOND, AND TO THE BEST OF OUR KNOWLEDGE REPRESENTS A POTENTIAL ERROR IN ALL OTHER WORK ON DIAMOND, since the embedded thermocouple method has not been employed by others. In addition, we have taken careful precautions

to eliminate heat transfer problems by the use of the colloidal graphite interface; in less well designed experiments, the temperature error could be even larger.

A cooling curve is also shown in Figure 7. As expected, during cooling the diamond temperature approaches the button heater temperature asympotically as the temperature falls.

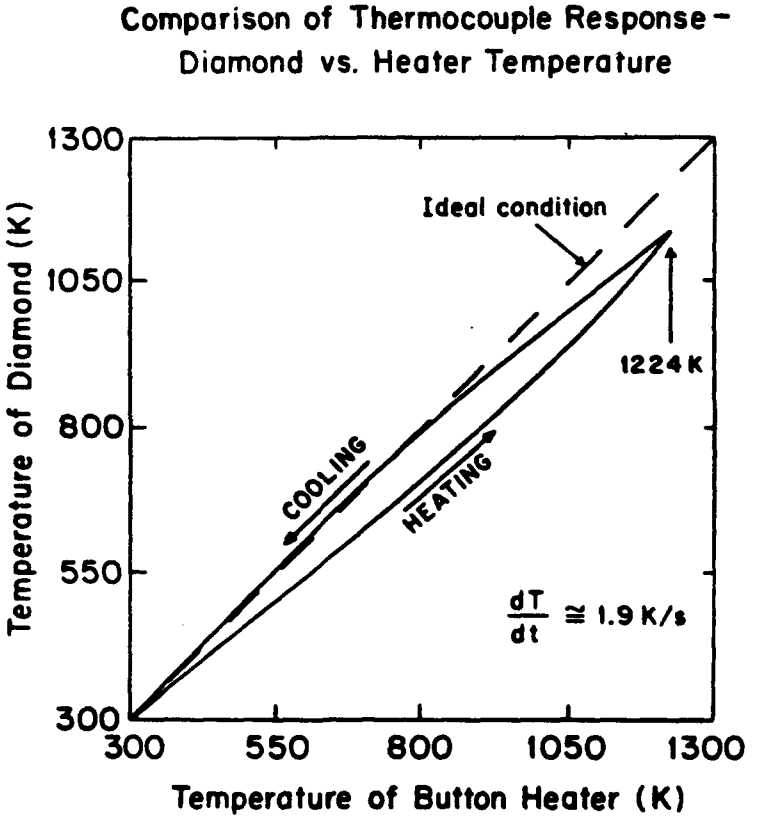

Figure 7. Comparison of Diamond Temperature and Button Heater Temperature during Programmed Heating and Cooling.

The performance of our temperature programming method is shown below in Figure 8, where the temperature versus time is plotted. A 1.9 K/s linear program has been applied to the crystal, and this program has been interrupted at two

preset temperatures where the controller maintains constant temperature.

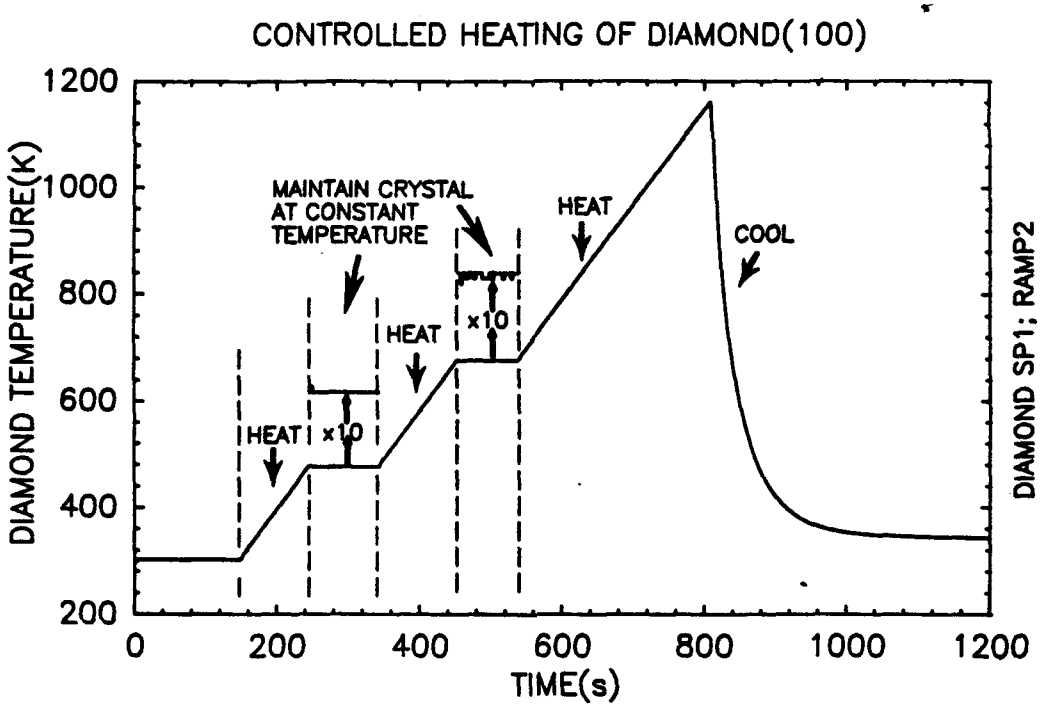

Figure 8. Temperature Programming of Diamond Single Crystal and Cooling.

Figures 6-8 illustrate that we have excellent control of the thermal behavior of the crystal, and that our measurements of the crystal temperature are likely to be correct.

F. Collimated Beam Dosers

These dosers contain an internal pinhole aperture which limits the flow of gas into the vacuum system [3]. The angular distribution of gas emitted by the dosers depends

upon the method of collimation. One of our dosers contains a capillary array, and the angular distribution of gas from this array has been determined theoretically [4,5].

The molecular beam dosers are calibrated with nitrogen gas, using the pressure drop in the calibrated-volume gas source region as a measure of the conductance through the apertures. The rate of flow measured for nitrogen may be applied to other gases using the Knudsen relationship, even though the storage pressure may be in the transition region between Knudsen and viscous flow, and this has been checked elsewhere [6].

The calibration of these dosers is shown in Figure 9. It may be seen that our pressure measurements are of high quality over time, and that the rate of effusion behaves as expected giving a plot of lnP which is accurately linear against time.

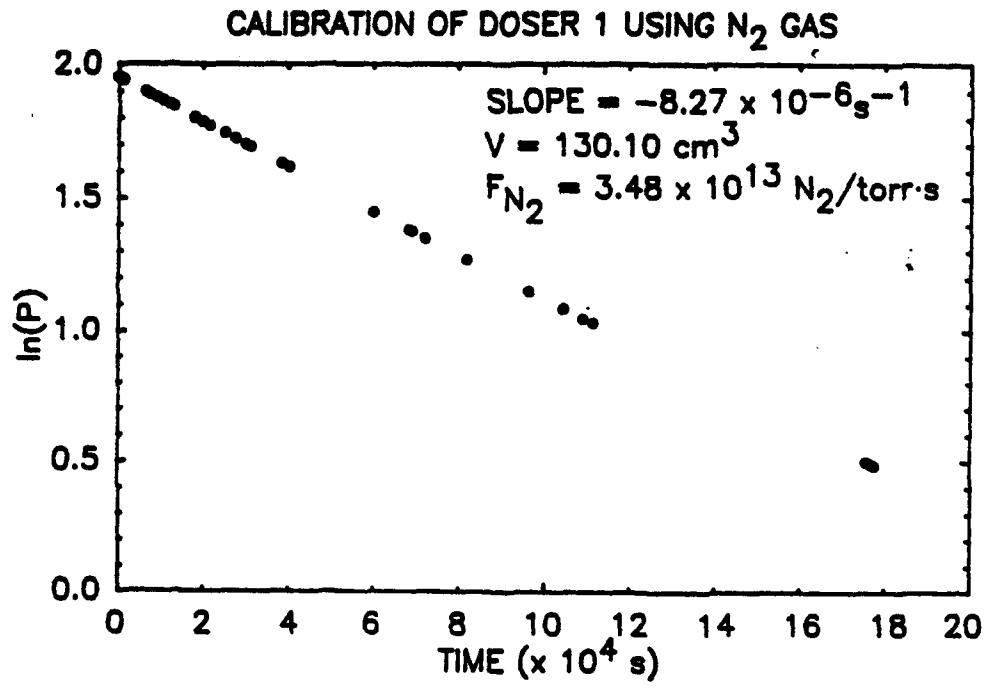

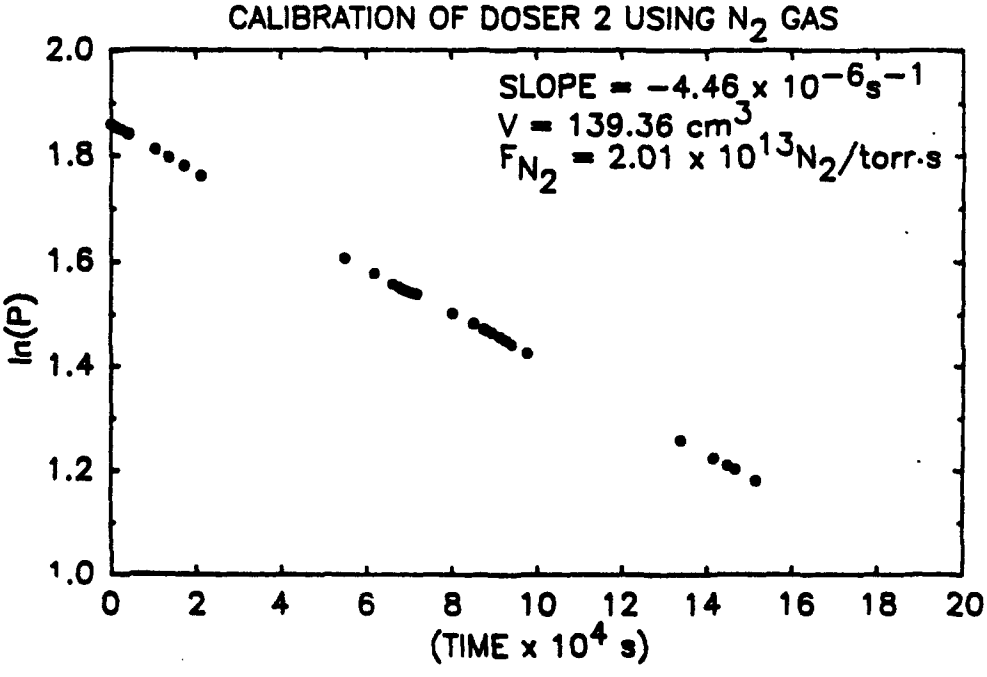

Figure 9. Calibration of Two Molecular Beam Dosers Using Nitrogen Gas.

G. Behavior of HREEL Spectrometer

The HREEL spectrometer is the most difficult of the surface measurement instruments to employ with a IIa diamond crystal. This is because of the small size of the diamond, the pickup of mechanical vibrations by the crystal holder, and surface charging of the insulator surface. We find, so far, that surface charging is not a major factor in preventing the use of this spectroscopy. Figure 10 illustrates this.

On the left hand side of the Figure 10, an elastic electron beam profile is shown. At a resolution of 65 cm^{-1}, a count rate of 3.2×10^4/s is observed, which is very acceptable for HREELS measurements. This elastic electron beam intensity is constant for many minutes as shown in region I of the figure, even though surface charging has occurred due to the electron beam. An ultraviolet lamp, passing only radiation below 3.5 eV, is turned on, and the elastic beam intensity drops as shown in region II. The ultraviolet lamp, by virtue of the photoexcitation of charge carriers in the diamond, is changing the electrostatic potential of the diamond surface, and detuning the HREELS spectrometer, causing the elastic beam intensity to fall. In region III, with the lamp off, the crystal electrostatically charges again to a constant surface potential, and the elastic beam intensity returns asympotically to its original value. These measurements suggest that acceptable HREELS measurements can be made on the diamond at a steady-state of constant surface charge without degradation of the resolution or significant alteration of the focal properties of the electron beam. It is interesting to note that control experiments, with photons having 3.5 eV or less energy, show that any photoelectrons produced in the HREELS instrument do not influence counting rates for scattered electrons.

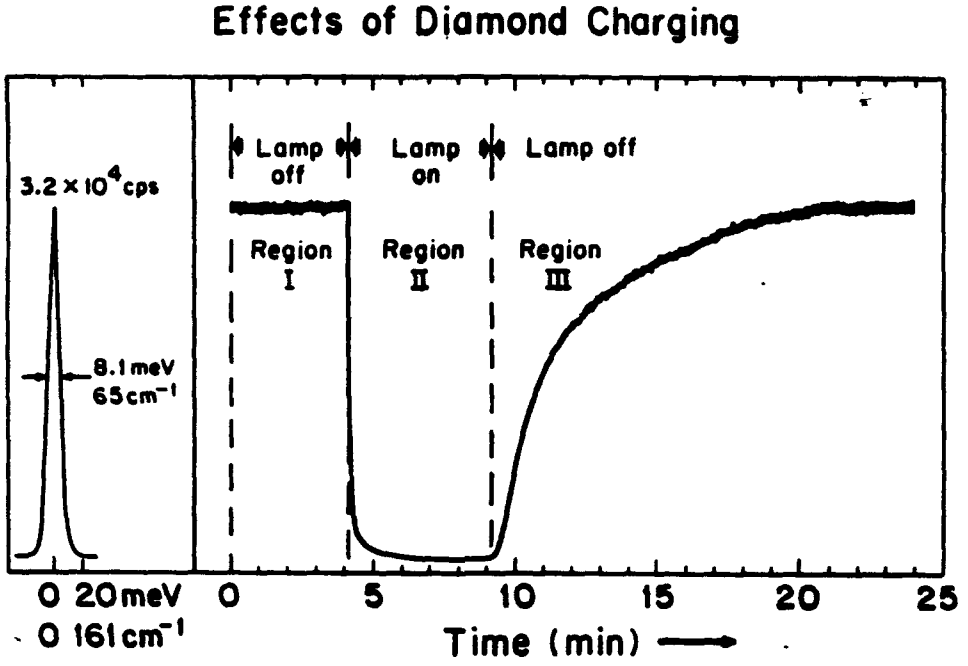

Figure 10. Effects of Electrostatic Charging of Diamond in the HREEL Spectrometer.

H. XPS Measurements of the Diamond(100) Surface

Figure 11 shows our first measurements of the diamond(100) surface using x-ray photelectron spectroscopy. An Al K_α source was employed. The solid line spectrum was obtained on the diamond(100) surface after heating to 1193 K. The dashed C(1s) spectrum was obtained after atomic deuterium adsorption. It may be seen that attenuation of C(1s) intensity occurs on the low binding energy side of the spectra when atomic D is adsorbed. This is in accordance with the involvement of a surface state on diamond(100) which is attenuated by deuterium adsorption, as seen also by Freedman et al. for fluorine adsorption on diamond(100) [7], and by Hsu and Turner [14].

The resolution of our measurements has not yet been optimized.

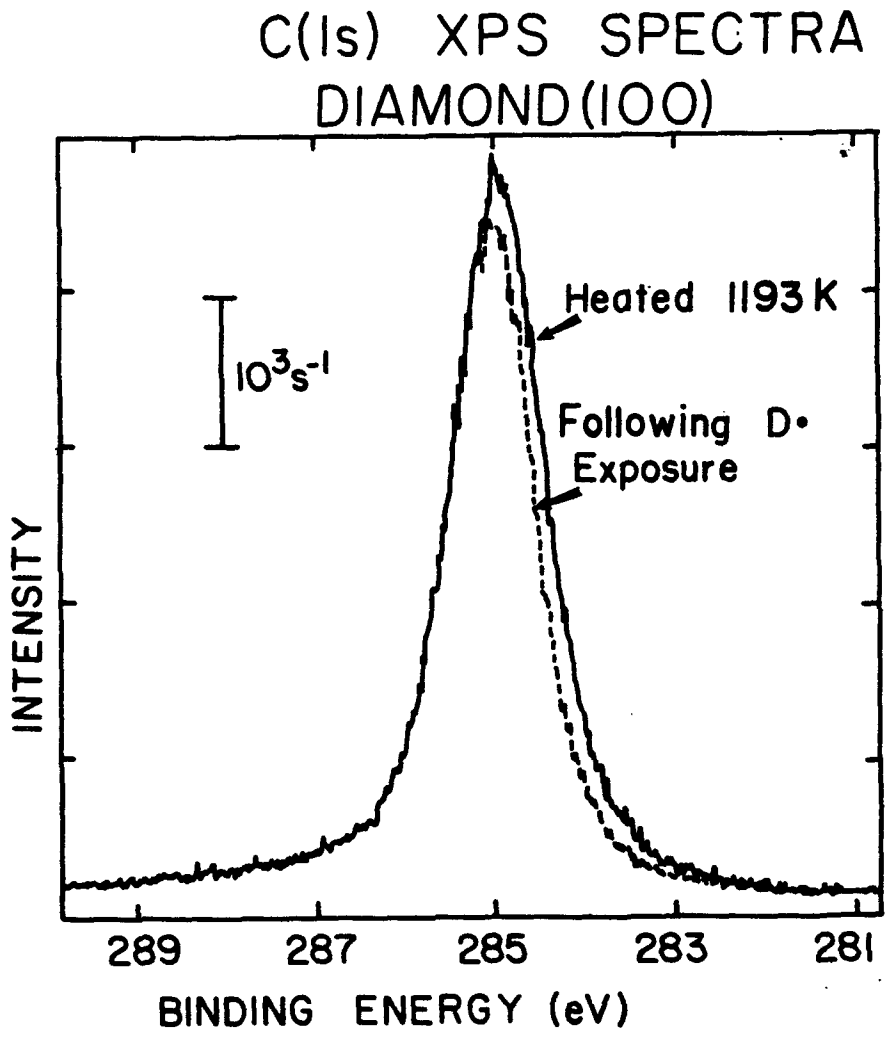

Figure 11. C(1s) XPS Spectra-Diamond(100).

I. Temperature Programmed Desorption from Diamond(100)

The diamond crystal was heated in ultrahigh vacuum to 1440 K for preliminary cleaning. It was then exposed to atomic D, produced on a hot tungsten filament, 4 cm away from the diamond, line-of-sight. A repeated thermal desorption experiment was carried out without further exposure to atomic D. The desorption experiment is discontinued in the early stages of hydrogen desorption. Figure 12 shows that all hydrogen isotopes are liberated

beginning near 1225 K and THAT REPEATED DESORPTION EXPERIMENTS CONTINUE TO EVOLVE HYDROGEN. This result must mean that atomic hydrogen or deuterium penetrates deeply into the diamond crystal and can then recombine with natural hydrogen present in the crystal bulk to produce HD. Diffusion effects from bulk to surface are evident in this repetitive experiment. These results are consistent with the report of Hamza, et al. [11b]. Our crystal has never been exposed to atomic H; hence the H_2 and HD are due to natural C-H bonding in the crystal.

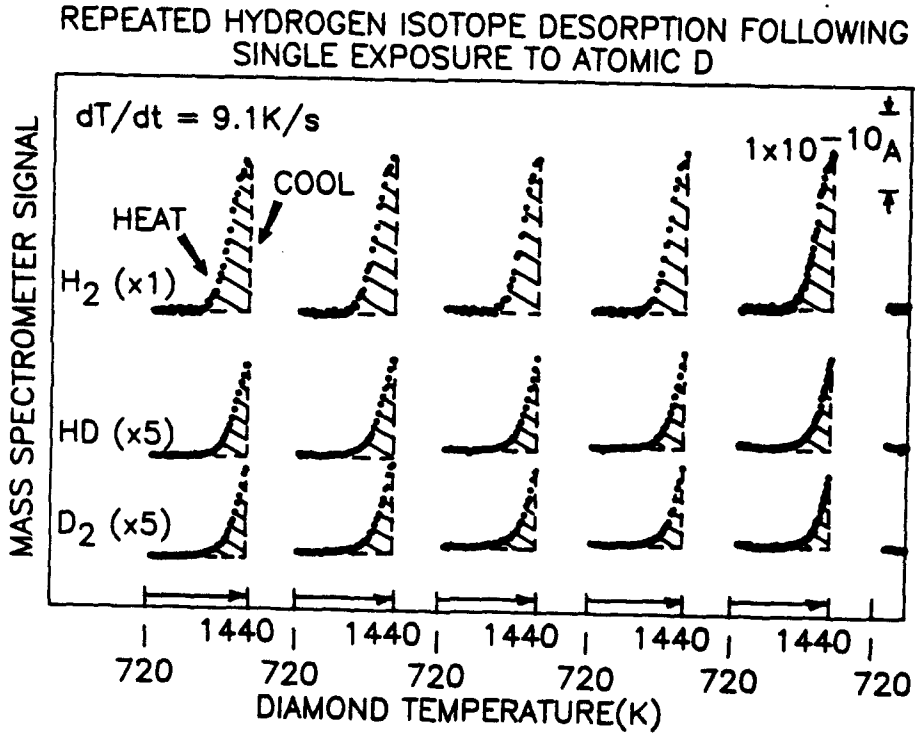

Figure 12. Temperature Programmed Desorption from Diamond(100), after exposure to Atomic Deuterium.

J. Atomic Force Microscopy (AFM) Studies of the Diamond(100) Crystal.

1. Topography of the Diamond(100) Crystal - AFM

One of the students working on this project (V.S. Smentkowski) carried out some exploratory work with Dr. Gary McClelland using the atomic force microscope (AFM) to probe the surface of the diamond(100) crystal. It was found that portions of the crystal exhibited atomically flat surfaces, as shown in the AFM scans in Figure 13.

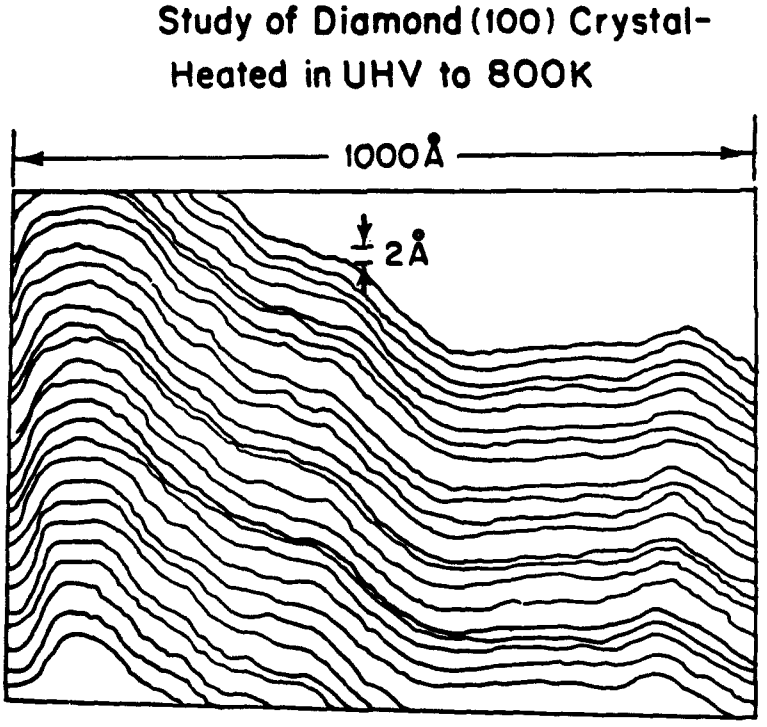

Figure 13. AFM scans of Diamond(100) Surface After Heating in Ultrahigh Vacuum at 800 K.

The AFM measurements were made with a tungsten tip containing a CVD grown diamond crystal, as shown in Figure 14. The continued presence of the diamond tip was confirmed by electron microscopy after the AFM measurements were completed.

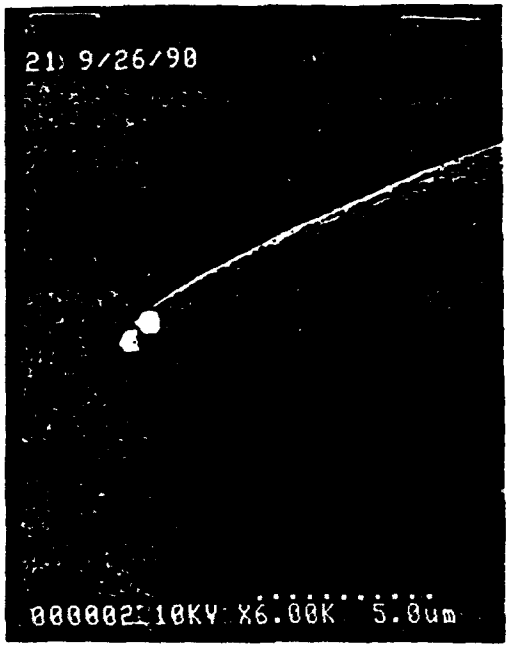

Figure 14. Diamond Coated AFM Tip Containing two Diamond Crystals.

2. Surface Friction Measurements - AFM

Friction measurements were also made, as shown in Figure 15. Here, the vertical axis is a measure of the lateral force (F_L) experienced by the AFM tip. As the tip is laterally moved (± 35 Å) along the diamond crystal surface, the normal force (F_N) applied to the tip (called the Load) is being systematically decreased as the tip is being withdrawn from the diamond surface.

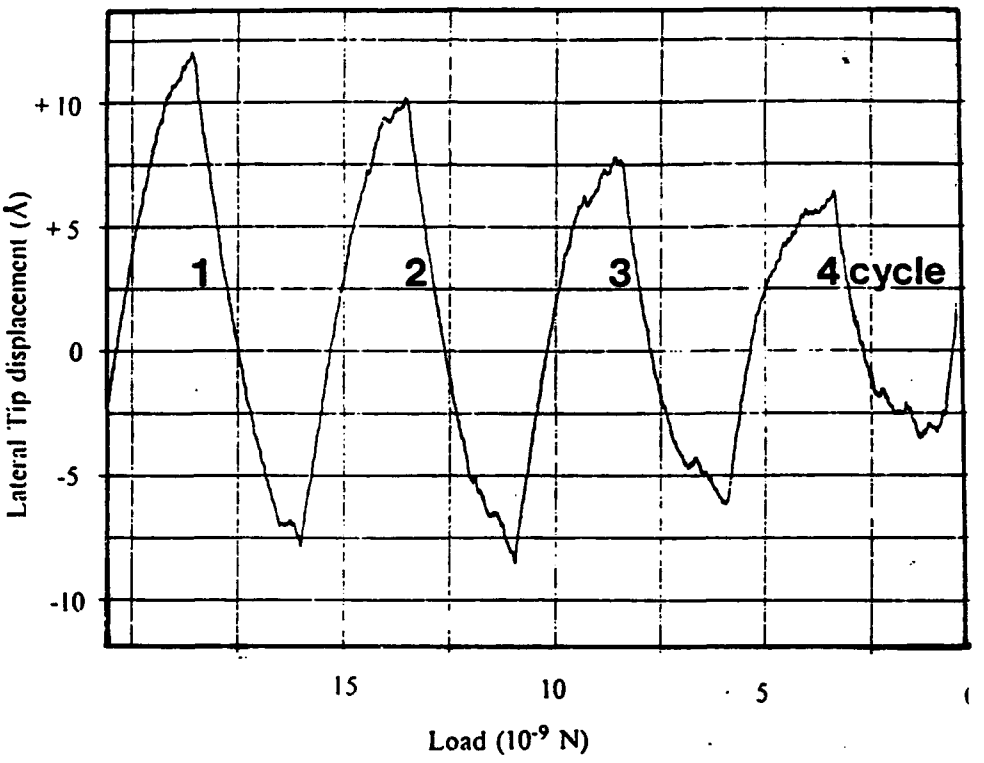

Figure 15. AFM Friction Loops for Diamond Sliding on Diamond(100).

For each cycle in the friction loops shown in Figure 15, the lateral frictional force may be calculated as one-half the peak-to-peak displacement (ΔD) times the lever force constant, 30N/m = 3 x 10^{-9} N/A.

The coefficient of friction, μ, is:

$$\mu = \frac{F_L}{F_N} = \frac{\Delta D \times 30\ N/m}{F_N}$$

In order to avoid systematic errors, a differential method is employed to calculate a more correct value of the coefficient of friction, $\langle\mu\rangle$, between cycles as follows:

$$\langle\mu\rangle = \Delta F_L/\Delta F_N,$$

where ΔF_L and ΔF_N are differential values throughout the experiment.

Thus, for each cycle we obtain a value of $\langle\mu\rangle$ as shown in the table below:

Cycle	$\langle F_N \rangle$	$\langle\mu\rangle$
1-2	15.2×10^{-9}	0.3
2-3	10.2×10^{-9}	1.5
3-4	5.2×10^{-9}	1.2

These preliminary results indicate the following physical features gleaned from the first diamond AFM measurements:

- The coefficient of friction is rather high between diamond surfaces.
- For repeated AFM measurements along the same track, the coefficient of friction approaches or exceeds unity after several cycles. This may be due to the production of nascent diamond surfaces as sliding occurs.

III. Proposed Research--Diamond(100).

A. Surface Chemistry of Hydrogen and Fluorine on Diamond(100).

Our previous proposal described a series of objectives in this area for the diamond(111) surface. The scientific part of this previous proposal is given in Section VI of this proposal. For reasons having to do with the availability of high quality diamond crystals, we chose to undertake our first studies on diamond(100) which can be

obtained with a better polished crystal face [10]. In addition, diamond(100) is less well studied than diamond(111). The objectives, fully described in our previous proposal (see Section VI), apply equally well to the diamond(100) surface, and are outlined below:

Objectives - Surface Chemistry of Diamond(100)

- Study the adsorption of atomic H, using LEED, TPD, XPS, ESDIAD, and HREELS methods.
- Look carefully for hydrogen-induced etching of diamond using line-of-sight TPD to observe desorption of possible hydrocarbon species.
- Study XeF_2 adsorption on clean and hydrogen - terminated diamond, leaving a fluorinated surface.
- Study the stability of hydrogenated and fluorinated diamond surfaces in vacuum and in the presence of oxidizing agents such as O_2, atomic O, and N_2O (a stronger oxidizing agent than molecular O_2).
- Study alternate ways to produce a fluorinated diamond surface by molecular adsorption of molecules such as C_2F_4, NF_3, and CF_3OF.
- Study the influence of fluorination on AFM behavior of diamond surfaces, in collaboration with Dr. Gary McClelland, IBM Almaden.

The apparatus which we have built is now being used for the first of these studies, and preliminary results have been reported in section II of this proposal.

B. Developments in Other Laboratories-Hydrogenation and Fluorination of Diamond(100) Surfaces.

During the 25 months of building time for our apparatus, our competition has been at work in the study of diamond(100) and its interaction with both H and F. These results are summarized below.

Hamza, Kubiak and Stulen have used LEED, TPD, and ESD methods, along with two photon photoemission to study the hydrogenation of diamond(100) [11b-12]. These results have been exciting and they have contributed to our understanding of diamond(100), as will be shown in Table I below. In addition, Thomas et al. [13] have studied the hydrogenation of diamond(100), as will be reported in the Table below. Finally, both Hsu and Turner [14] and Freedman and

Stinespring [7] have studied the fluorination of diamond, using XeF_2 [diamond (111)] [14], or atomic fluorine [diamond(100)] [7].

Table I. Hydrogen Chemisorption-Diamond(100).

Property Measured	Hamza, et al. [11b]	Thomas, et al. [13]
1. Hydrogen saturation coverage.	>10 ML*	1ML
2. LEED pattern change from (1 x 1) → (2 x 1) on desorbing H_2.	yes	no
3. Desorption Temperature of H_2.	1120 K (low coverage) 920 K (high coverage)	1223 K (all coverages)
4. Other Thermal Desorption Products	none	$\cdot CH_3$ C_2H_2
5. ESD Products	H^+ H_2^+ C^+ CH^+ O^+	not studied

*H_2 is reported to originate from the bulk

The comparison of the results obtained in Table I indicates that significant differences exist between the results from laboratories studying hydrogen adsorption on

diamond(100). The special experimental methods to be employed in our work (line-of-sight TPD; microchannelplate LEED detection to avoid e-beam damage; direct measurement of diamond crystal temperature; HREELS) should help to resolve the controversies indicated in Table I.

The work on fluorination of diamond(100) by Freedman and Stinespring [7] was carried out using XPS and LEED as the measurement tools. A discharge source was employed to deliver fluorine atoms to the diamond. The clean diamond exhibited a (1 x 1) LEED pattern. The C(1s) XPS peak contained a shoulder on the low binding energy side which was assigned as a surface state, shifted 1.1 eV below the bulk C(1s) binding energy. Adsorption of F attenuated this state, and produced a shoulder 1.8 eV above the bulk C(1s) binding energy, in agreement with earlier results on diamond(111) [8,9]. Using XPS, the F(1s) binding energy is about 686 eV. This fluorine layer disappears in the range 700 K - 1000 K, by an unknown depletion process, as measured by XPS.

C. Proposed Work on Hydrogenation and Fluorination of Diamond(100).

The above results are considered to be a good start, but much remains to be done. Table II lists experiments which need to be carried out in our laboratory to add to existing knowledge, as well as to help to resolve controversies.

Table II. Experimental Needs in Understanding the Chemistry of H and F on Diamond(100).

H/Diamond(100)

Need	Comment
1. Line-of-sight TPD	The desorption of H_2 and D_2 needs to be remeasured. Coverage needs to be studied. Does hydrogen come from the bulk?

	Need	Comment
		Desorption kinetics need to be studied.
		Unusual hydrocarbon products need to be studied.
2.	LEED	Question of role of surface impurities on (1x1)→(2x1) reconstruction needs to be carefully addressed.
3.	ESDIAD	H^+ ion emission directions need to be determined.
		Origin of two types of H^+ having different kinetic energies [11b] needs study.
4.	HREELS	No information in literature on diamond(100) using HREELS.

F/Diamond(100)

	Need	Comment
1.	Line-of-sight TPD	The desorbing species need to be identified; are there CF_x species?
2.	LEED	(2 x 1) surface needs to be studied.
3.	ESDIAD	F^+ ion beam directions as indicators of C-F bond directions need to be studied.

	Need	Comment
4.	HREELS	Vibrational spectra need to be studied to determine the chemical nature of the CF_x species.
5.	Fluorinated molecule/ adsorption	All work previously proposed needs to be done.
6.	XeF_2 + H/diamond(100)	All work previously proposed needs to be done.
7.	Stability of F/diamond (100) to oxidation at extreme conditions of temperature and oxidizing potential	All work previously proposed needs to be done.
8.	AFM studies	Comparison of clean diamond(100) to F/diamond(100) needs to be done.

The 12 areas of investigation in Table II form the core of our experimental objectives for the next three years. The apparatus to achieve the majority of these objectives is completed and is working well in all respects. As shown earlier in this proposal, preliminary measurements, using the two surface spectroscopies, XPS and HREELS, have been made in this apparatus which is dedicated to the study of the diamond surface. In addition, preliminary atomic deuterium adsorption studies have been done, as shown earlier.

IV. Outline of Progress in Electron Stimulated Desorption.

A. Research Activities - Electron Stimulated Desorption

Work supported by AFOSR involving the digital ESDIAD (electron stimulated desorption ion angular distribution) apparatus was discontinued during this funding period, but a

number of papers have been produced under AFOSR support, during this period.

B. Summary of Publication Activities

A total of 12 papers or reviews have been published or submitted during the 25 months of this project. The titles and references of these contributions are listed below:

* A. Szabó, M. A. Henderson, and J. T. Yates, Jr., "Evidence for Anisotropic Vibration of Diatomic Adsorbate - NO and CO Chemisorbed on Stepped Pt(111)," J. Chem. Phys. 92, 2208 (1990).

* M. Kiskinova, A. Szabó, and J.T. Yates, Jr., "Dynamical Effects during CO-induced Phase Transformation in p(2x2)S and p(2x2)Se Overlayers on Pt(111)," Vacuum 41, 82 (1990).

* J. T. Yates, Jr., A. Szabó, M. Kiskinova, and M. A. Henderson, "Dynamics of Adsorbate Interactions on Single Crystal Surfaces," Proceedings of the 10th Anniversary of the Japanese Surface Science Society, (1989).

* M. A. Henderson, R. D. Ramsier and J. T. Yates, Jr. "Photon- versus Electron-Induced Decomposition of $Fe(CO)_5$ Adsorbed on Ag(111) - Iron Film Deposition," J. Vac. Sci. Technol. A 9(3), 1563 (1991).

* V. S. Smentkowski and J. T. Yates, Jr. "Selected Bibliography - Diamond Surface Chemistry," AFOSR Unclassified Technical Report (Project No. 2303).

* R.D. Ramsier and J.T. Yates, Jr., "Electron Stimulated Desorption: Principles and Applications", Surface Science Reports, Volume 12, Nos. 6-8 p. 243-378, (1991).

* R.D. Ramsier and J.T. Yates, Jr., "Electron Stimulated Desorption and its Application to Chemical Systems", in "Dynamics of Gas-Surface Collisions, Eds. M.N.R. Ashford and C.T. Rettner, Royal Society of Chemistry, Cambridge, (1991).

* J.T. Yates, Jr., A. Szabó, and M.A. Henderson, "The Influence of Surface Defect Sites on Chemisorption and Catalysis", Division of Petroleum Chemistry, American Chemical Society Symposium "Structure in Heterogeneous Catalysis", Boston, April 1990.

* R.D. Ramsier, M.A. Henderson and J.T. Yates, Jr., "Electron Induced Decomposition of $Ni(CO)_4$ on Ag(111)", accepted, Surface Science.

* M.A. Henderson, R.D. Ramsier and J.T. Yates, Jr., "Minimizing Ultrahigh Vacuum Wall Reactions of $Fe(CO)_5$ by Chemical Treatment of the Dosing System", accepted, Journal of Vacuum Science and Technology.

* M.A. Henderson, R.D. Ramsier and J.T. Yates, Jr., "Low Energy Electron Induced Decomposition of $Fe(CO)_5$ Adsorbed on Ag(111)", accepted, Surface Science.

* M.A. Henderson, A. Szabó and J.T. Yates, Jr., "One-Dimensional CO Island Formation in the Coadsorption of H_2 and CO on the Steps of Pt(112)", submitted to Surface Science.

C. Summary of the Highlights of Recent Papers Concerned with Electron and Photon Induced Processes on Surfaces.

The 9 nonreview publications outlined in section B above fall into two separate categories. The first category concerns the use of the digital ESDIAD method to observe unusual adsorption phenomena on a Pt(112) single crystal surface containing periodic step defects. The second category of work concerns the behavior of adsorbed metal carbonyls when irradiated with either electrons or ultraviolet photons. This second activity is of importance in writing metal film patterns on electronic devices.

1. Adsorbate Dynamics on Stepped Pt(112).

The structure of the Pt(112) surface is shown in Figure 16. It consists of three atom wide terraces of Pt(111) planes, separated by monatomic steps having a Pt(100) orientation. These crystals can be prepared by cutting at an angle of 19.5° from the Pt(111) direction. LEED studies of the cleaned and annealed crystal confirm that the expected periodicity is present.

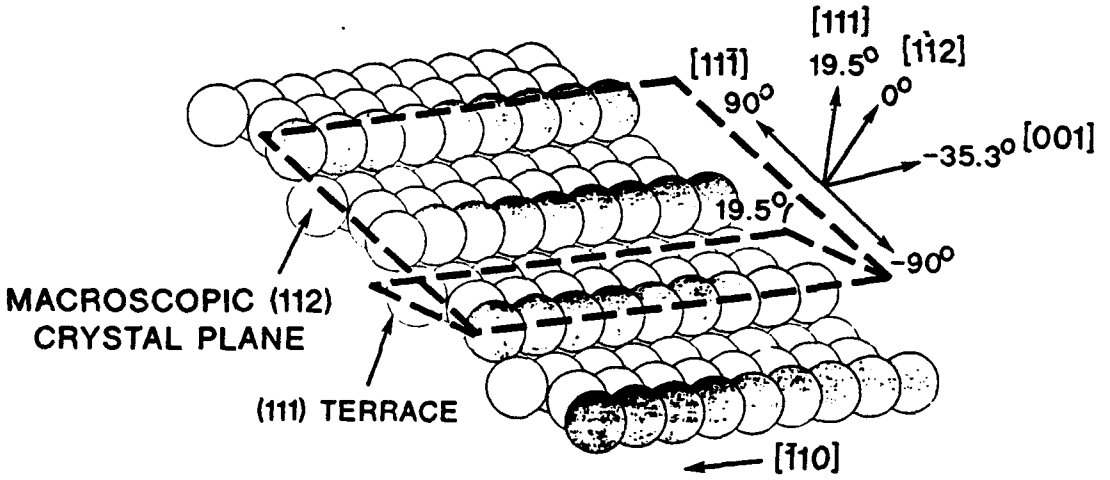

Figure 16. Structure of the Pt(112) Surface [15].

It is well known that NO tends to bind to Pt surfaces in a bridge-bonded fashion. Furthermore, preferential bonding to step sites is expected at low coverages, by analogy to the behavior of other adsorbing molecules such as CO and O_2. Thus, it would be expected that bridged NO species, bound to two Pt atoms through the N atom in NO would be formed at low coverages on the step sites of the Pt(112) surface. But to which Pt atoms will the NO bond at the step? This question is answered quite nicely by the use of the digital ESDIAD technique to image the trajectories of desorbing O^+ ions from adsorbed NO, produced by electron stimulated desorption. Figure 17 shows the O^+ ESDIAD patterns obtained at various crystal temperatures. A fin-shaped O^+ ESDIAD pattern is observed, yielding an elliptical cross sectional pattern as shown in Figure 17. The width of the ESDIAD pattern will be determined by the amplitude of the low frequency thermal motions of the adsorbate, and as expected, this width increases with increasing crystal temperature, as seen in Figure 17.

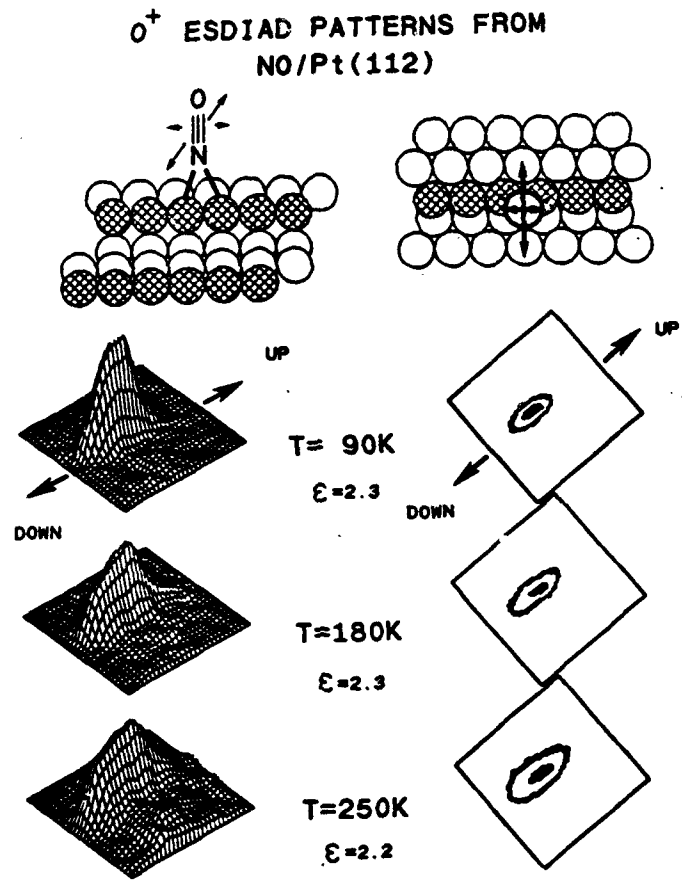

Figure 17. ESDIAD Patterns from NO Adsorbed on Pt(112) [16].

The long axis of the elliptical cross section is accurately perpendicular to the step edge. This indicates that low frequency vibrations (frustrated translations) of the NO molecule are of higher average amplitude in the upstairs-downstairs directions than in the directions parallel to the step edge. This observation is consistent with bridged bonding of NO to pairs of Pt atop step atoms, causing the plane of the Pt_2NO species to be parallel to the step edge, as shown in Figure 18. Based on molecular dynamics considerations, the amplitude of the vibrations perpendicular to the molecular plane should be larger than vibrations in the plane of the surface complex, as indicated qualitatively by the arrows on the top view of the stepped surface in Figure 17 [16]. Thus, digital ESDIAD has

determined the particular bonding structure of NO on a defect step site, through the observation of the NO molecule's characteristic dynamical behavior.

2. Comparison of Reactive Chemistry on Step and Terrace Sites.

The ability to preferentially place molecules on the step sites of the Pt(112) surface has permitted an unusual experiment to be performed in which the model reaction between adsorbed CO and adsorbed oxygen has been probed [17]. Through a series of thermal treatments devised for this experiment, it has been possible to place either $^{12}C^{16}O$ or $^{12}C^{18}O$ on the step sites in the presence of the opposite CO isotope on the terrace site. The Pt(112) crystal also contains a fraction of a monolayer of chemisorbed atomic oxygen. The reaction between the oxygen and the CO is monitored by mass spectrometry during temperature programming of the crystal. Figure 18 shows the schematic results of this experiment, where it has been found that below ~ 200 K, THE ISOTOPIC CO PRESENT ON THE TERRACE SITES PARTICIPATES EXCLUSIVELY IN THE PRODUCTION OF $CO_2(g)$.

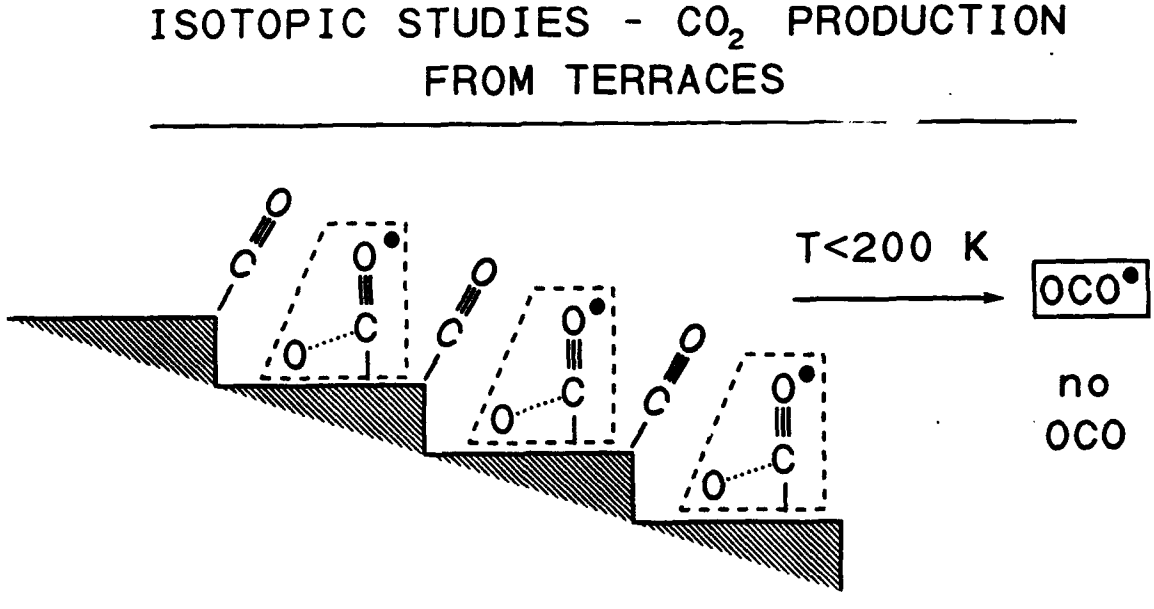

Figure 18. Site Distribution of CO Isotopes on Pt(112) and Observed Isotopic CO_2 Production [17].

The experimental CO_2-production data is shown in Figure 19. Below ~ 200 K, isotopically pure CO_2, involving the isotopic CO adsorbed specifically on the terrace sites, is produced. Above 200 K, diffusion of isotopically labeled CO from its original site of adsorption prevents obtaining information from this kind of experiment.

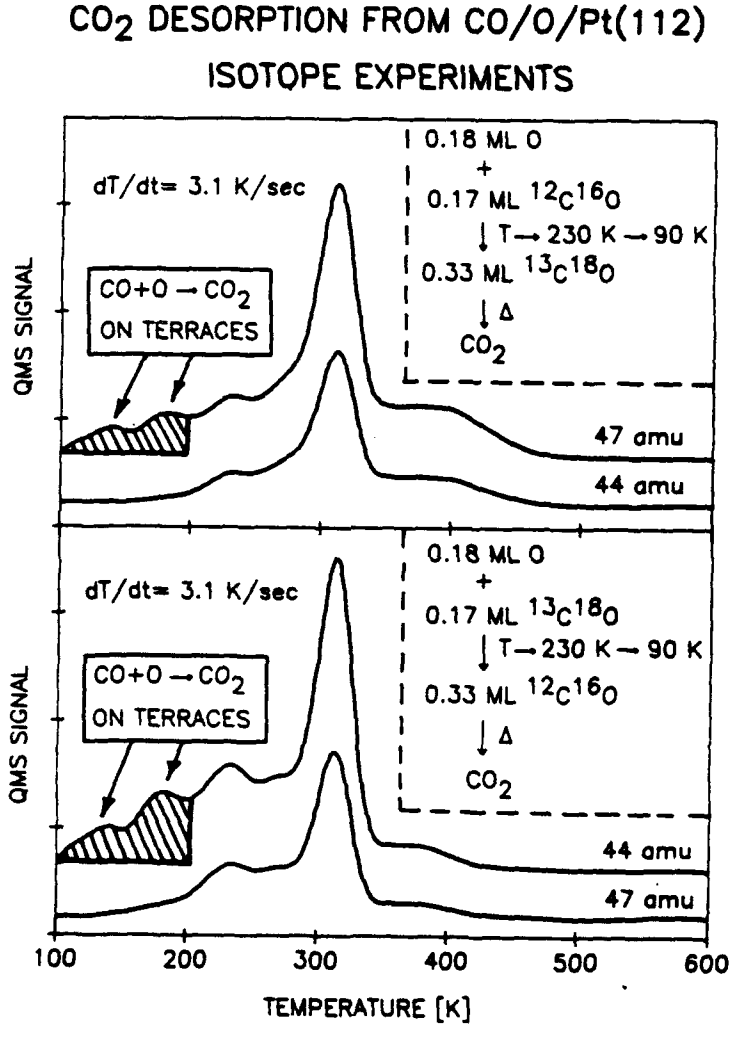

Figure 19. Production of Isotopic CO_2 Species from the CO(a) + O(a) Reaction on Pt(112) [17].

This is the first isotopic adsorbate site labeling experiment to be performed on a single crystal surface

containing periodic defect sites. The experiment indicates that the lower binding energy of CO on the terrace sites, compared to the step sites, may be responsible for the higher reactivity of CO on the terrace sites.

3. One Dimensional CO Island Dynamics on Pt(112)

Previous studies have shown that the chemisorption of CO on Pt(112) occurs preferentially on the step sites, and that the CO molecules undergo a series of transformations in bonding angles as the coverage increases in the one dimensional islands [15,18]. The discrete transformations in tilt angles of the CO molecules are related to changing steric effects between the CO molecules which occur as the fraction of empty sites along the steps decreases as the CO coverage increases. These observations have given a detailed picture of the behavior of the interacting CO molecules which has not been possible using other surface science techniques; ESDIAD is able to measure the tilt angles for the CO to 1° accuracy.

The CO-CO interactions are not observed at low coverages on the steps, and CO molecules in this condition adsorb with the M-CO orientation being 20° in the downstairs direction. As the coverage increases, repulsive interactions between CO molecules cause lateral tilting parallel to the step edge direction, resulting in ± 13° tilt angles along the step edge directions. This configuration occurs at three-fourths coverage of the steps, and is a result of CO tilting toward neighboring empty step sites. As the coverage is increased still further on the step sites, and the empty sites become filled, the steric repulsions cannot cause lateral tilting, and an orthogonal tilt pattern develops where the CO molecules sterically avoid each other by tilting upstairs and downstairs with an M-CO bond angle difference of 38°. All of these measurements are made using a neutral metastable desorbing species, CO^*, which does not suffer the image effects of departing ions produced in ESD, so that the CO escape directions measured are likely to be close to the true M-CO bond angles present at the moment of excitation. Figure 20 shows the sequence of ESDIAD patterns measured as a function of coverage on Pt(112), and Figure 21 shows the structural model proposed to explain the ESDIAD behavior.

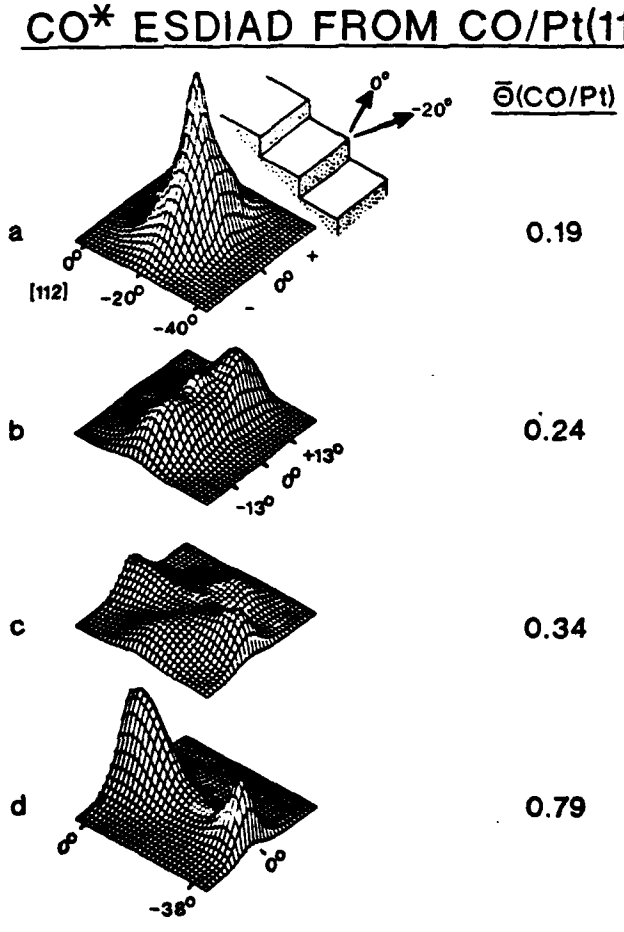

Figure 20. CO* ESDIAD Patterns for Increasing CO Coverage on Pt(112) [15].

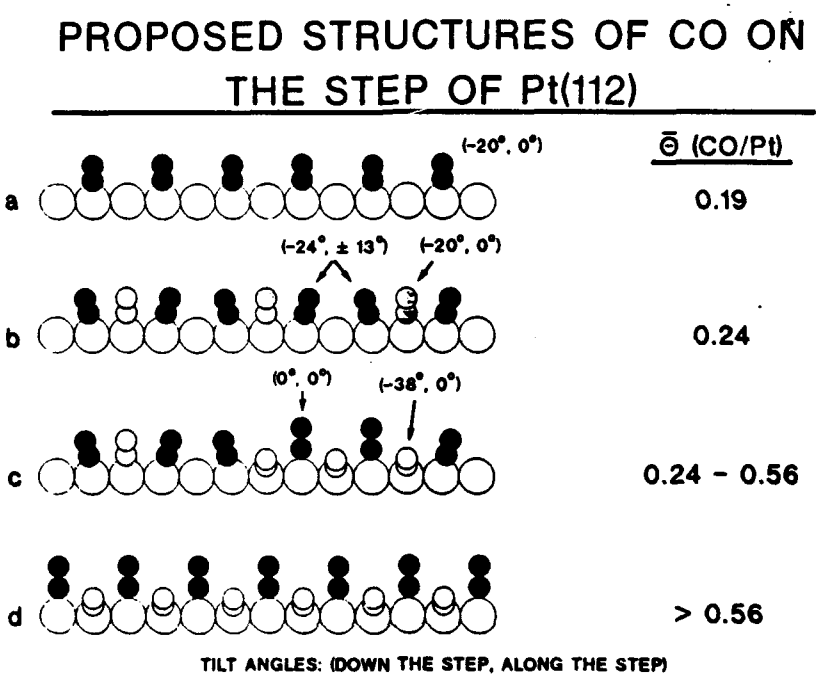

Figure 21. Proposed Tilting Structures for Various Coverages of CO on Pt(112) [15].

We have now found that low coverages of CO on the Pt(112) steps may be pushed through the same set of tilting configurations by the coadsorption of hydrogen onto the surface containing only 0.04 monolayers of CO. This means that hydrogen and CO both adsorb on step sites and that repulsive H-CO interactions exist. It is likely that one dimensional CO islands are produced in contact with one dimensional H islands. Although immiscible two dimensional islands have been observed on smooth (111) surfaces before [19], this is the first example of such an effect in <u>one dimension</u>. A diagram of the structural situation for mixtures of adsorbed H and CO is shown in Figure 22.

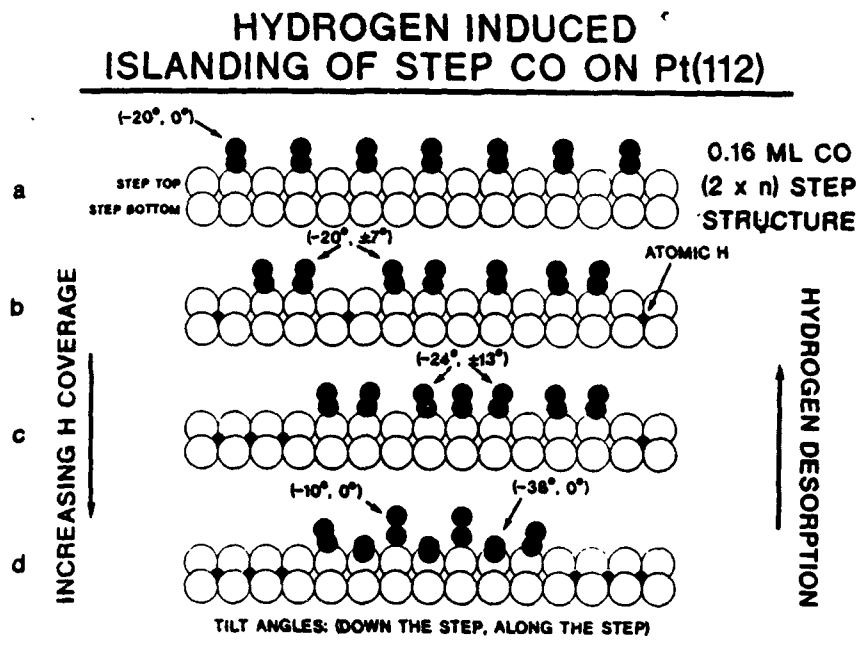

Figure 22. One Dimensional CO and H Islands Formed on the Steps of Pt(112)- H Atoms Occupy Four Fold Hole Sites on the Step Face, while CO Occupies Atop Sites on the Steps [20].

4. Electronic Excitation and Dissociation of Adsorbed Metal Carbonyls.

The behavior of transition metal carbonyls upon electronic excitation while adsorbed on a surface can form the basis for the "writing" of metal films on semiconductor surfaces [21]. This is potentially of importance in the fabrication of electronic devices.

We have carried out studies of electron-induced and photon-induced decomposition of the metal carbonyls, $Fe(CO)_5$ and $Ni(CO)_4$ on a Ag(111) surface. Ag(111) is inactive for the adsorption of CO at the temperature of these experiments. The purpose was to determine the relative efficiency of electrons and photons for making pure metal films, and also to characterize the nature of the metal deposits produced.

In order to do this work, layers of the metal carbonyl were adsorbed on Ag(111) at low temperatures. Temperature

programmed desorption indicated that both monolayer and multilayer carbonyls were present. No chemical decomposition of the carbonyl was observed.

When either electrons or ultraviolet photons interact with the metal carbonyl, it is observed that the layer is depleted, and that conversion to metal clusters containing one or more carbonyl groups occurs. These metal clusters liberate CO(g) near 300 K, and then remain on the silver surface. Figure 23 shows the temperature programmed desorption experiments for $Fe(CO)_5$ following the use of both 256 nm photons and 132 eV electrons.

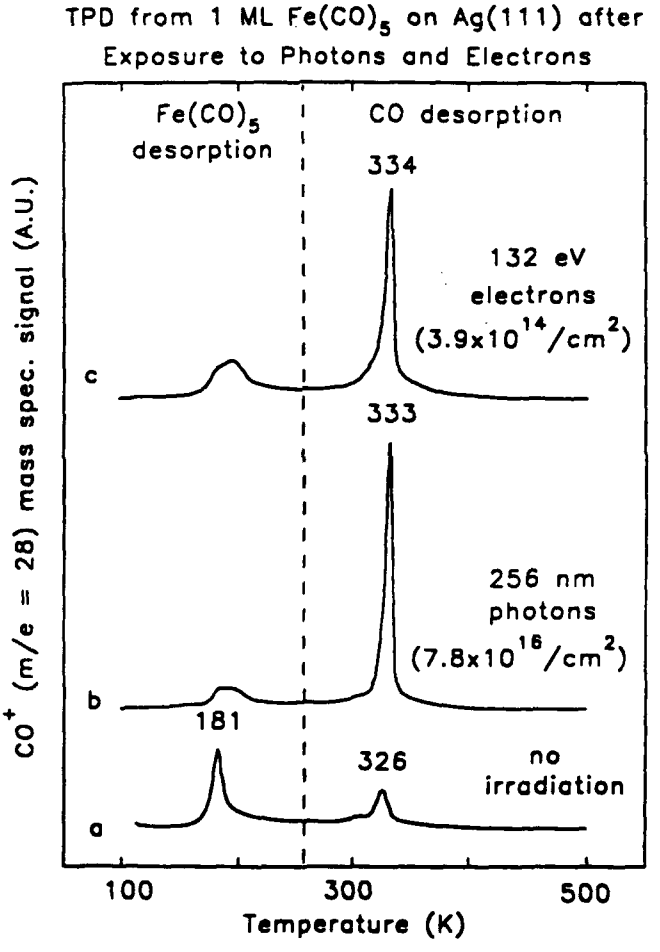

Figure 23. **Temperature Programmed Desorption from 1 ML $Fe(CO)_5$ on Ag(111) after irradiation with photons or electrons [21]. The CO desorption peak near 330 K originates from iron clusters containing adsorbed CO, which are produced by the irradiation. The small amount of this in the nonirradiated experiment is related to thermal decomposition of $Fe(CO)_5$ on Ag defect sites.**

The cross section for electron beam decomposition varies from 1 A^2 to 14 A^2 (3eV - 132 eV). In contrast, the photon cross section is several orders of magnitude smaller.

In addition to irradiation by electrons in the 3 eV - 132 eV range, some studies with 2 keV electrons were also performed. It was found that only small amounts of carbon or oxygen were deposited on the iron clusters for the low energy electrons and for the photons. In contrast, the 2 keV electrons resulted in considerable impurity deposition. Thus, for the deposition of clean Fe films at the highest efficiency, our studies indicate that low energy electrons will be most efficient.

A VERY INTERESTING OBSERVATION WAS MADE CONCERNING THE METAL CLUSTERS PRODUCED BY PHOTOLYSIS. THESE CLUSTERS ARE INACTIVE FOR THE ADSORPTION OF CO AT PRESSURES USED IN ULTRAHIGH VACUUM EXPERIMENTS. Since the bulk metals, Fe and Ni, are active for chemisorption of CO, we conclude that the clusters produced by this photolytic means are so small as to be nonmetallic.

Similar studies have been done with $Ni(CO)_4$ on Ag(111), and similar conclusions are reached [22-23]. Recently, this work has been confirmed in Professor Wilson Ho's laboratory, where photodecomposition studies of this type were performed on Ag surfaces and on graphite [24].

V. References

1. R.A. Rudder, J.B. Posthill and R.J. Markunas, Electronics Letters, 25, 1220 (1989).

2. R.J. Muha, S.M. Gates, P. Basu and J.T. Yates, Jr., Rev. of Scientific Instruments, 56, 613 (1985).

3. M.J. Bozack, L. Muehlhoff, J.N. Russell, Jr., W.J. Choyke, and J.T. Yates, Jr., J. Vac. Sci. Technol., A5, 1 (1987).

4. C.T. Campbell and S.M. Valone, J. Vac. Sci. Technol., 13, 408 (1985).

5. A. Winkler and J.T. Yates, Jr., J. Vac. Sci. Technol., A6, 2929 (1988).

6. C.C. Cheng, R.M. Wallace, P.A. Taylor, W.J. Choyke, and J.T. Yates, Jr., J. Appl. Phys., 67, 3693 (1990).

7. A. Freedman and C.D. Stinespring, Appl. Phys. Lett., 57, 1194 (1990).

8. J.F. Morar, F.J. Himpsel, G. Hollinger, J.L. Jordan, G. Hughes, and F.R. McFeely, Phys. Rev. B33, 1340 (1986).

9. J.F. Morar, F.J. Himpsel, G. Hollinger, J.L. Jordan, and G. Hughes, Phys. Rev. B33, 1346 (1986).

10. Private communication, Dr. Harris, Dubbeldee Harris.

11. (a) A.V. Hamza, G.D. Kubiak and R.H. Stulen, Surf. Sci., 206, L833 (1988); (b) Surf. Sci., 237, 35 (1990).

12. G.D. Kubiak and K.W. Kolasinski, Phys. Rev. B39, 1381 (1989); J. Vac. Sci. Technol., A6, 814 (1988).

13. R.E. Thomas, R.A. Rudder and R.J. Markunas, paper presented at ECS Conference, May 1991.

14. D.S.Y. Hsu and N.H. Turner, 4th SDIO/IST Technology Initiative Symposium, Crystal City, VA.

15. M.A. Henderson, A. Szabó, and J.T. Yates, Jr., J. Chem. Phys., 91, 7255 (1989).

16. A. Szabó, M.A. Henderson, and J.T. Yates, Jr., J. Chem. Phys., 92, 2208 (1990).

17. J.T. Yates, Jr., A. Szabó, and M.A. Henderson, Division of Petroleum Chemistry, ACS Symposium "Structure in Heterogeneous Catalysis," Boston, April 1990; also paper in progress.

18. M.A. Henderson, A. Szabó, and J.T. Yates, Jr., Chem. Phys. Lett., 168, 51 (1990).

19. E.D. Williams, P.A. Thiel, W.H. Weinberg, and J.T. Yates, Jr., J. Chem. Phys., 72, 3496 (1980).

20. M.A. Henderson and J.T. Yates, Jr., submitted, J. Chem. Phys.

21. See references [1-16] in M.A. Henderson, R.D. Ramsier, and J.T. Yates, Jr., J. Vac. Sci. Technol., A9, 1563 (1991).

22. R.D. Ramsier, M.A. Henderson, and J.T. Yates, Jr., accepted Surf. Sci.

23. M.A. Henderson, R.D. Ramsier, and J.T. Yates, Jr., accepted Surf. Sci.

24. S.K. So and W. Ho, J. Chem. Phys., 95, 656 (1991).